CHELATES OF ZINC(II) AND CADMIUM(II) WITH 2-(2-THIAZOLYLAZO)-4-METHOXYPHENOL*

V. KUBÁŇ and L. SOMMER

Department of Analytical Chemistry,
J. E. Purkyně University, 611 37 Brno

Received June 14th, 1974

Complex equilibria of 2-(2-thiazolylazo)-4-methoxyphenol with zinc(II) and cadmium(II) in 30% v/v ethanol were studied spectrophotometrically, combining graphical and numerical methods. Purple-blue ML chelates (λ_{max} 598 nm, ε_{max} 18 000, $\log \beta_{11} = 5{\cdot}6$ for Zn^{2+} and λ_{max} 600 nm, ε_{max} 18000, $\log \beta_{11} = 5{\cdot}3$ for Cd^{2+}) and ML_2 chelates (λ_{max} 600 nm, $\varepsilon_{max} \simeq 31000$, $\log \beta_{12} \simeq 13{\cdot}7$ for Zn^{2+} and λ_{max} 600 nm, $\varepsilon_{max} \simeq 31500$, $\log \beta_{12} \simeq 13{\cdot}3$ for Cd^{2+}) are formed in the solutions: the latter predominate in solutions with excess ligand. The Zn(II) and Cd(II) chelates with heterocyclic *o*-hydroxy-substituted azo-dyes are not very suitable for the spectrophotometric determination of these metals.

In the previous papers[1,3] the acid–base properties of 2-(2-thiazolylazo)-4-methoxyphenol (TAMP) and its complex equilibria with mercuric and nickel(II) ions were studied in detail. During the interpretation of these systems, a combination of graphical and numerical methods for handling absorbance curves proved advantageous, based on the linear least squares method and on the general method of minimization of the sum of the squares of the deviations between the experimental and theoretical absorbance values. Similar methods have been employed in this work to study systems of TAMP with cadmium(II) and zinc(II) ions.

EXPERIMENTAL

Reagents and Apparatus

The 2-(2-thiazolylazo)-4-methoxyphenol (TAMP) substance was from the Institute of Pure Chemicals, Lachema, Brno. The content of the active component in the dye was determined by elemental analysis (C, H, N) and the purity of the substance was checked using thin-layer chromatography on the MN-Kieselgel G silica. It was found that the substance was chromatographically pure. Stock solutions were prepared by dissolving the crystalline substance in a small amount of dimethylformamide and 1M-NaOH and by diluting with water or ethanol.

Stock solutions of zinc and cadmium nitrates, with concentrations of $c_M = 0{\cdot}4912$M-$Zn(NO_3)_2$ and $0{\cdot}4802$M-$Cd(NO_3)_2$ were prepared by dissolving the doubly recrystallized p.a. substances in $0{\cdot}1$M-HNO_3. The solutions were standardized gravimetrically and by EDTA-titrations and were diluted with $0{\cdot}1$M-HNO_3.

* Part III in the series Some 2-(2-Thiazolylazo)-4-methoxyphenol Complex (TAMP) Equilibria; Part II: This Journal *40*, 604 (1975).

The ionic strength of the solutions was maintained at a value of $I = 0{\cdot}10$ by combining the appropriate volumes of HNO_3, KNO_3 or NaOH. The procedure for the measurement of various experimental dependences has been described in detail in a previous paper[1]. The pH values in 30% v/v ethanol were not corrected and are denoted by the pH symbol in the present paper.

The ethanol used contained 5% v/v methanol. The other chemicals were commercial substances of *p.a.* purity; some of them were purified by recrystallization, distillation, *etc.*

The solution acidity was measured with a PHM 4k pH-meter (Radiometer, Denmark), using a G 202B glass electrode and a K 401 saturated calomel electrode. The instrument scale was standardized using a phosphate (Radiometer, S 1001, $pH_{25\,°C} = 6{\cdot}48$), a phthalate (NBI, $pH_{25\,°C} = 4{\cdot}01$) and a borate (NBI, $pH_{25\,°C} = 9{\cdot}18$) buffer.

All spectrophotometric measurements were performed using an SF D2 single-beam spectrophotometer (LOMO, USSR) at a constant temperature, $t = 25{\cdot}00 \pm 0{\cdot}05$°C, in a special apparatus for spectrophotometric measurements in a nitrogen atmosphere[1,4]. The spectra were recorded on a UNICAM SP 700 double-beam recording spectrophotometer at 25°C.

Methods

In order to determine the basic characteristic of the complexes — the absorption maximum position, the molar absorption coefficient, the stoichiometry and the equilibrium or conditional constant — graphical interpretation of the absorbance curves was carried out, employing slope-intercept transformations, $A = f(F_i)$ or $A = f(G_i)$, and graphical logarithmic analysis using the $\log F = f(pH)$, $\log F = f(-\log c_M)$ or $\log F = f(-\log c_L)$ dependences combined with a numerical method based on the linear least squares method (PRCEK type programs).

Using the criterion of the linearity of $A = f(F_i)$ or $A = f(G_i)$ dependences, the stoichiometry of the complexes and the most probable reaction mechanism were found; from the slopes and the intercepts of the appropriate linear dependences the equilibrium constants and the molar absorption coefficients were then determined. The principles and the fundamental equations for the two methods were given earlier[1].

The results are complemented by the values of the equilibrium constants and by the numbers of protons dissociated, obtained from the graphical logarithmic analysis of the absorbance curves and of the curves for the dependence of the absorbance on the concentration of a particular component. Some ambiguous reaction mechanisms were verified or excluded by the method of corresponding solutions, plotting the $pH_{0i} = f(-\log c_M)$ dependences. The stoichiometry of the complexes was also verified employing the method of continuous variations under selected experimental conditions.

RESULTS

Chelates of Zinc (II)

Several pronounced absorption maxima are found in the spectra of Zn(II) solutions in 30% v/v ethanol containing TAMP, measured at pH values from 1 to 9 and at various concentration ratios ($c_M/c_L = 100$; 10; 1; 0·1); maxima at 470 and 370 nm correspond to the molecular form of ligand LH and those at 598–600 and 386 to 390 nm to the purple-blue chelate of Zn^{2+} with TAMP. The long-wave absorption band of the chelate (Fig. 1) is somewhat distorted on the side of longer waves, but the splitting of the two absorption bands, similar to that encountered with nickel (II) chelates with TAMP (ref.[1]), is absent here.

TABLE I

Optical Characteristics of the Complex Species of Zinc(II) Ions with TAMP in 30% v/v Ethanol $I = 0{\cdot}10$, $t = 25{\cdot}00°C$, $c_L = 4{\cdot}912 \cdot 10^{-5}$M.

c_M/c_L	$10^{-3} \cdot \nu_{max}$ cm^{-1}	$10^{-3} \cdot \nu_i$ cm^{-1}		λ_{max}, nm		λ_i, nm	$10^5 \cdot c_L$ mol/l
100	25·6	16·7	19·6	390	599	510	4·912
100[a]				386	596	511	4·912
10	25·6	16·7	19·6	390	599	510	4·912
1	25·6	16·65	19·5	390	598	512	4·912
1/10[c]	—	16·65	19·5	—	600	510	24·56
5·75[b]	25·6	16·7	19·6	386	600	510	4·912
5·75[b a]				387	596	511	4·912
Mean	*25·6*	*16·7*	*19·6*	*389*	*599*	*510*	

[a] Measured on the SF D2 spectrophotometer, [b] spectra at a constant pH of 5·75, in dependence on the cation concentration, [c] $c_M = 2{\cdot}456 \cdot 10^{-5}$M.

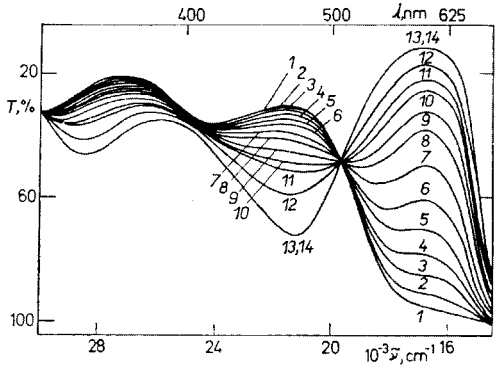

FIG. 1

The Absorption Curves for Zn(II) Solutions with TAMP

$c_M/c_M = 100$, $c_M = 4{\cdot}912 \cdot 10^{-3}$M, 30% v/v ethanol, $I = 0{\cdot}10$, $t = 25{\cdot}0°C$, $d = 10$ mm. Curve — pH: *1* 3.29, *2* 3·71, *3* 3·87, *4* 4·04, *5* 4·22, *6* 4·45, *7* 4·67, *8* 4·83, *9* 4·96, *10* 5·13, *11* 5·41, *12* 5·57, *13* 6·21, *14* 6·68.

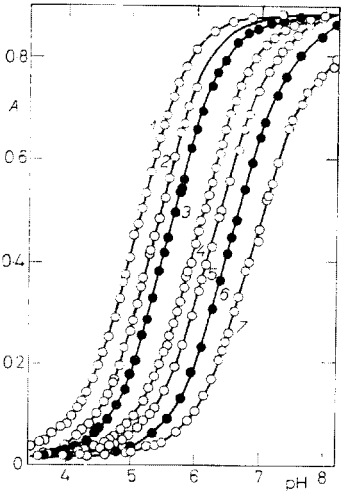

FIG. 2

The Absorbance–pH Curves for Zn(II) with TAMP, for Various Ratios c_M/c_L

For the conditions see Fig. 1, $c_L = 4{\cdot}912 \cdot 10^{-5}$M, 595 nm. Curve — c_M/c_L: *1* 100, *2* 50, *3* 30, *4* 10, *5* 5, *6* 3, *7* 1.

TABLE II

A Survey of the Average Values of the Logarithm of the Equilibrium Constant for the Zn^{2+} Chelates with TAMP Under Various Experimental Conditions

c_M/c_L	$-\log {}^*\beta_{mn}$	$-\log {}^*\beta_{mn}{}^a$	$-\log {}^*\beta_{mn}{}^b$	q	$r_{xy}{}^a$	$-\log {}^*\beta_{mn}{}^a$	$r_{xy}{}^b$	$-\log {}^*\beta_{mn}{}^b$	q
	pH_{inf}	graphical methods			the PRCEK program				
100	2·76	2·74	2·73	0·998	0·9947	2·7402 ± 0·0100	0·9926	2·7224 ± 0·784	0·9221
50	2·74	2·74	2·75	0·985	0·9986	2·7320 ± 0·0239	0·9974	2·7173 ± 0·0285	0·9925
30	2·75	2·77	2·75	0·992	0·9915	2·7322 ± 0·0167	0·9951	2·7391 ± 0·1063	0·9866
10	2·74	2·72	2·73	0·990	0·9982	2·7291 ± 0·0265	0·9987	2·7273 ± 0·0590	0·9939
5	2·70	2·71	2·74	0·988	0·9926	2·7313 ± 0·0355	0·9954	2·7237 ± 0·0683	0·9789
3	2·74	2·72	2·75	0·988	0·9990	2·7338 ± 0·0205	0·9995	2·7327 ± 0·0199	0·9965
≧3	2·74	2·73	2·74	0·990	0·9957	2·7337 ± 0·0222	0·9965	2·7271 ± 0·0584	0·9787
1	2·58	2·58	2·60	0·997	0·9951	2·5760 ± 0·0975	0·9978	2·5823 ± 0·3965	0·9670
1/2	2·67	2·70	2·72	0·989	0·9936	2·7121 ± 0·1572	0·9976	2·7538 ± 0·2319	1·0224
1/5	2·87	2·87	2·86	1·040	0·9930	2·8672 ± 0·1372	0·9969	2·8425 ± 0·2978	1·2247
1/10	2·90	2·92	2·93	1·030	0·9944	2·9533 ± 0·2245	0·9974	2·9384 ± 0·0722	0·9707
6·0[a]	—	—	—	1·0	0·9958	2·7366 ± 0·1083	0·9972	2·7368 ± 0·1211	1·0121
6·0$_d$	—	—	—	2·0	0·9939	2·9847 ± 0·3846	0·9949	2·9905 ± 0·2679	1·9587

[a] The results of direct graphical analysis using the $A = f(F_i)$ and $A = f(G_i)$ transformations, [b] the results of the graphical logarithmic analysis of the lof $F = f(pH)$ dependence, [c] concentration dependences $A = f(c_M)$, [d] dependences $A = f(c_L)$.

In the spectra of equimolar solutions and solutions with excess ligand, the absorption bands of the anionic form of the ligand, L^- (λ_{max} = 560 – 570 nm), appear in a weakly alkaline region, in addition to the absorption bands of the LH form, which are present in acidic and neutral media. Absorption by the two ligand forms distorts the absorption bands of the chelate and renders the measurement impossible at λ values below 500 nm.

The spectra at a constant pH of 5·75, with varying c_M/c_L concentration ratios, are analogous to those for excess zinc(II) ions and the position of the absorption maxima virtually does not change. Only curves for $c_M/c_L \geqq 5$ pass through an isosbestic point at λ_i 510 nm, while the other curves pass through a diffuse isosbestic point at 505 nm. Curves for excess ligand are again affected by the absorption of the LH form.

TABLE III

A Survey of the Average Values of the Molar Absorption Coefficient for the Zn^{2+} Chelates with TAMP Under Various Experimental Conditions

λ	Direct		Graphical		PRCEK program	
	ε_1	ε_2	ε_1	ε_2	ε_1	ε_2
470[a]	9 030	2 735	9 080	2 715	9 027 ± 30	2 739 ± 34
560[a]	860	14 855	830	14 500	808 ± 60	14 325 ± 64
580[a]	425	17 460	540	17 285	442 ± 62	17 158 ± 72
595[a]	295	17 940	265	18 030	244 ± 62	17 998 ± 71
610[a]	160	17 305	165	17 225	188 ± 74	16 577 ± 84
630[a]	90	15 430	120	15 170	88 ± 58	14 760 ± 63
470[b]	17 900	7 750	17 755	7 950	17 816 ± 128	7 920 ± 122
580[b]	2 000	30 500	2 010	30 670	1 946 ± 99	30 873 ± 136
595[b]	500	31 000	625	31 240	876 ± 152	31 069 ± 210
610[b]	50	30 000	75	29 950	138 ± 82	29 820 ± 109
630[b]	0	26 500	0	26 050	0 ± 87	26 200 ± 887
650[b]	0	21 900	0	21 750	0 ± 113	21 487 ± 152
470[c]	9 200	2 550	9 320	2 420	9 175 ± 88	2 598 ± 97
560[c]	820	14 900	880	15 010	883 ± 63	15 126 ± 73
580[c]	450	17 500	505	17 420	497 ± 59	17 553 ± 49
595[c]	250	18 100	275	18 210	248 ± 73	18 203 ± 78
610[c]	100	17 450	115	17 330	142 ± 66	17 428 ± 67
630[c]	50	15 600	0	15 330	22 ± 83	15 127 ± 46

[a] The results form the absorbance–pH curves for $c_M/c_L \geqq 3$, $\varepsilon_1 \equiv \varepsilon_L$, [b] the results from the absorbance–pH curve for $c_L/c_M = 10$, $\varepsilon_1 \equiv \alpha\varepsilon_L + \varepsilon_{ML}$, [c] the results from concentration dependences $A = f(c_M)$ for a pH range of 4·0–6·0.

Two sharp isosbestic points on the spectra indicate simple transition of the ligand molecular form, LH, to the purple-blue chelate of Zn^{2+} with TAMP. The optical characteristics of the Zn^{2+} chelate with TAMP under various experimental conditions are surveyed in Table I.

The absorbance–pH curves of solutions of Zn^{2+} with TAMP for various concentration excesses of zinc ions ($c_M/c_L = 100 - 3$) and a constant ligand concentration, $c_L = 4{\cdot}912 \cdot 10^{-5}$M, indicate unambiguously that a single complexation equilibrium occurs, as they are quite symmetrical and are shifted to more acidic values within pH 3·5–8·0 with increasing cation concentration. Well-developed horizontal parts on the absorbance–pH curves show that the complex is formed quantitatively even in solutions with small concentration excesses of the cation (Fig. 2).

The shape of the absorbance–pH curves for solutions with ratios of $c_M/c_L = 100 - 3$ and for wavelengths of 470, 560, 580, 595, 610 and 630 nm permitted direct determination of the values of $A_{01} = \varepsilon_1 c_L$ or $\varepsilon_L c_L$ and $A_{02} = \varepsilon_2 c_L$ and thus also the calculation of the molar absorption coefficient values, ε_L and ε_2, and an appropriate assessment of the values of the logarithm of the equilibrium constant from the position of the inflexion point on the $A = f(pH)$ curve. The A_{01} and A_{02} values were used as the initial values for the graphical interpretation of the curves and for their interpretation using the PRCEK Program.

For plotting the slope-intercept transformations, $A = f(F_i)$ and $A = f(G_i)$, for various concentration excesses, the values of variables F_i and G_i calculated and printed out after the first computing cycle of the PRCEK program were used advantageously. Because of the tediousness of their construction, the plots were constructed for only a single wavelength, λ 595 nm, with various concentration excesses and the complexation equilibria considered,

$$M + LH \rightleftarrows ML + H \quad (111), \qquad (A)$$

$$M + 2\,LH \rightleftarrows ML_2 + 2\,H \quad (122), \qquad (B)$$

$$M + 2\,LH \rightleftarrows ML_2H + H \quad (112), \qquad (C)$$

$$2\,M + LH \rightleftarrows M_2L + H \quad (211), \qquad (D)$$

$$2\,M + 2\,LH \rightleftarrows M_2L_2 + 2\,H \quad (222), \qquad (E)$$

$$2\,M + 2\,LH \rightleftarrows M_2L_2H + H \quad (212). \qquad (F)$$

where the numbers in parentheses correspond to the coefficients of the general complexation equilibrium

$$mM + nLH_x \rightleftarrows M_mL_nH_{nx-q} + qH \quad (mqn)\,{}^*\beta_{mn}. \qquad (G)$$

The plot of the $A = f(F_i)$ dependence for a hundredfold excess of zinc ions and $c_L = 4{\cdot}912 \,.\, 10^{-5}$M is given in Fig. 3. Only the $A = f(F_i)$ curves for the reaction coefficients $mqn = 111$ and $mqn = 211$, *i.e.* for equilibria (A) and (D) are perfectly linear. An analogous situation is found for all the other concentration ratios and wavelengths.

The molar absorption coefficients ε_1 and ε_2 and the equilibrium constants $^*\beta_{11}$, obtained graphically for the wavelength given above, had the same values as those obtained using the PRCEK program after the first iteration; therefore, these values were further determined employing the least squares method and the first computing cycle of the PRCEK program. In this way the tedious plotting of the above transformations and graphical determination of the intercept and slope were completely eliminated. Part of the results is given in Table II and III. The slope of the dependence (the equilibrium constant) varies only minutely for various experimental conditions and the values of the intercepts on the y-axis (ε_L or ε_2) are also constant within experimental error (Table II and III).

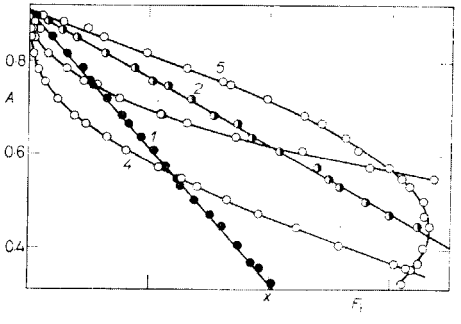

FIG. 3

Graphical Interpretation of the Absorbance–pH Curves of Zn(II) Solutions with TAMP

30% v/v ethanol, $c_M/c_L = 100$, $c_M = 4{\cdot}912 \,.\, 10^{-3}$M, the other conditions are identical with those given in Fig. 1. Curve — *mqn* coefficients — the F_i value at point X — reaction: *1* $111 - 1{\cdot}10^{+3} - M + LH = ML + H$, *2* $211 - 1{\cdot}10^{+3} - 2\,M + LH = M_2L + H$, *3* $222 - 2{\cdot}10^{+7} - 2\,M + 2\,LH = 2\,H$, *4* $122 - 1{\cdot}10^{3} - M + 2\,LH = ML_2 + 2\,H$, *5* $112 - 3{\cdot}10^{-2} - M + 2\,LH = ML_2H + H$.

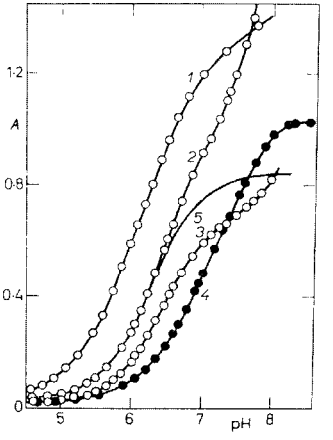

FIG. 4

The Absorbance–pH Curves for Zn(II) Solutions with TAMP for Various c_L/c_M Values

$c_M = 2{\cdot}456 \,.\, 10^{-5}$M, for the other conditions see Fig. 1. Curves — $c_L/c_M = \lambda$: *1* 2—630 nm, the pH-axis shifted by one unit, *2* 10—595 nm, *3* 10—650 nm, *4* 2 to 650 nm, *5* $A - A_L = f(pH)$ — 10—595 nm (calculated).

The A_{01} and A_{02} values on the two horizontal parts of the absorbance-pH curves were used for graphical logarithmic analysis employing the log $F = f(pH)$ dependences. These dependences were always linear with a slope close to unity. The values of the logarithm of the equilibrium constant and of the slope (the number of protons dissociated, q) are given in Table II and III.

The method of corresponding solutions for curves with a constant ligand concentration, $c_L = 4{\cdot}912 \cdot 10^{-5}$M, and increasing concentration of zinc ions, $c_M = 1{\cdot}5 \cdot 10^{-5} - 5 \cdot 10^{-3}$M, excludes the presence of polynuclear complexes of the $M_mL_nH_{nx-q}$ type, since the slope of the $pH_{oi} = f(-\log c_M)$ plot equals unity ($m/q = 1$).

The data were handled by the PRCEK program for the given conditions, under the same assumptions as for the graphical analysis. The most probable mechanism was selected for a wavelength of 595 nm and complexation equilibria $(A)-(F)$.

TABLE IV

A Survey of the Values of the Correlation Coefficient, r_{xy}, and the Sum of the Squares of Deviations U for Reaction Mechanisms $(A)-(J)$ and Solutions of Zinc(II) Ions with TAMP
t 25°C, I 0·10, λ 595 nm, $c_L = 4{\cdot}912 \cdot 10^{-5}$M.

c_M/c_L	mqn	r_{xy}	$10^2 \cdot U$	r_{xy}^c	c_M/c_L	mqn	r_{xy}	$10^2 \cdot U$	r_{xy}^c
100	111	·99945	·6472	·99969	50	111	·99673	9·656	·99883
	112	·85116	104·05	·64139		112	·78807	440·5	·85683
	121	·89745	795·6	·93581		121	·48640	436·8	·61589
	211	·99945	·6472	·99969		211	·95385	16·92	·98478
	122	·97587	1 839	·73681		122	·95925	4 805	·80818
	212	·84635	1 364	·64134		212	·78943	457·3	·86141
	222	·97661	11 123	·73663		222	·95660	640·2	·82620
10	111	·99894	·1067	·99979	1	111	·99548	·4167	·99809
	112	·97623	530·6	·92399		112	·70574	1 517	·87285
	121	·88750	397·4	·75674		121	·81258	811·4	·94339
	211	·99799	·1221	·99455		211	·91402	1 001	·97614
	122	·97383	311·0	·86757		122	·68268	2 146	·63311
	212	·98497	535·1	·96558		212	·47308	1 734	·97624
	222	·87040	9 380	·85925		222	·29573	1 440	·83767
1/10[a]	111	·99432	·2223	·99883	1/10[ab]	111	·99756	9·687	·99892
	112	·60066	167·92	·60507		112	·69652	308·0	·80424
	121	·86825	55·27	·97831		121	·87224	15·34	·96632
	122	·96866	18·17	·47152		122	·97342	11·98	·54869
	221	·74356	647·9	·67056		221	·73566	79·64	·65789
	133	·52349	64 397	·42443		133	·49965	70 197	·48467

[a] $c_L = 4{\cdot}912 \cdot 10^{-4}$M, [b] 650 nm, [c] the value obtained by the graphical logarithmic analysis.

The sums of the squares of the deviations, U, and the correlation coefficients r_{xy} after the first computing cycle are given in Table IV. The lowest U values and r_{xy} values closest to unity were found for molar reaction coefficients $mqn = 111$ and $mqn = 211$, confirming the conclusion drawn from the graphical method that the most probable reaction course is represented by equilibrium (A) or (D). The latter equilibrium was again excluded using the method of corresponding solutions, since the log $*\beta_{11} = f(\log c_M)$ dependence is linear.

The whole set of absorbance–pH curves for excess cation was then handled for coefficients $mqn = 111$ and all the wavelengths, employing the full number of iterations, $N_i \leqq 6$, necessary to obtain the required agreement between successive A_{01} or A_{02} values. Changes in the values of the quantities with varying experimental conditions are negligible within experimental error. Part of the results is given in Table II and III.

The interpretation of the absorbance–pH curves for equimolar solutions and solutions containing excess ligand (Fig. 4) is considerably complicated by the ligand dissociation ($pK_{a2} = 8{\cdot}328$) and by absorption of the anionic form, L^- ($\lambda_{max} \simeq$ $\simeq$ 570 nm, $\varepsilon_{max} \simeq 16000$). The wavelength region used for the measurements was therefore shifted to a long-wave spectral region ($\lambda > 610$ nm), where the second horizontal branch of the $A = f(pH)$ curve was at least slightly perceptible.

The curves were again graphically analyzed only for 595 and 650 nm and ligand concentration excesses $c_L/c_M = 1$ and 10. The $A = f(F_i)$ or $A = f(G_i)$ dependences for the above equilibria, (A)–(F), and for newly considered equilibria

$$M + 3\,LH \rightleftarrows ML_3H_{3-q} + qH\,, \quad (1q3) \quad q = 1, 2, 3 \qquad (H)$$

$$ML + LH \rightleftarrows ML_2 + H\,, \qquad (I)$$

$$ML + LH \rightleftarrows ML_2H\,, \qquad (J)$$

taking into account the ligand dissociation,

$$LH \rightleftarrows L + H \quad (011) \qquad (K)$$

are almost linear for coefficients $mqn = 111$, *i.e.* for equilibrium (A) or (I). The graphical logarithmic analysis of the curves indicates non-linearity of the $\log F = f(pH)$ curves in virtually the whole pH range, the slope being approximately $q = 1{\cdot}3$ (Fig. 5).

Similar results were obtained by using the PRCEK program for these curves; the best U and r_{xy} values for $mqn = 111$ and 211 were found using equimolar solutions

and those for $mqn = 111$ and 122 using solutions with excess ligand, *i.e.* for equilibria (A) and (D) or (A), (I) and (B), respectively. The set of data with $c_L/c_M = 1$, 2, 5 and 10 and wavelengths of 470, 560, 580, 595, 610, 630, 650 and 670 nm was treated for coefficients 111 and 122. The values of the characteristic quantities (r_{xy}, U, ε, $\log {}^*\beta_{mn}$ *etc.*) vary considerably with changes in the experimental conditions; the best results were obtained for wavelengths $\lambda > 610$ nm and for higher ligand excesses, $c_L/c_M = 10$. This indicates the simultaneous existence of two equilibria, (A) and (I). These equilibria are also encountered, together with the ligand dissociation, when the values of the molar absorption coefficient, ε_1, on the first horizontal portion of the curve are compared for solutions with excess zinc ion and with excess ligand. The former ε_1 values are the molar absorption coefficient of the HL form of the ligand ($\varepsilon_1 = 264$, 202, 197, 253, 323 and 227 for $c_M/c_L = 100$, 50, 30, 10, 5 and 3, respectively, at λ 595 nm), while the latter, which should correspond to the metal or the first complex, ML, attain substantially higher values (359, 603 and 876 for $c_L/c_M = 1$, 2 and 10, respectively), probably due to absorption by the second complex. The ε_2 values for the higher complex are about twice the ε_1 values at the same wavelengths.

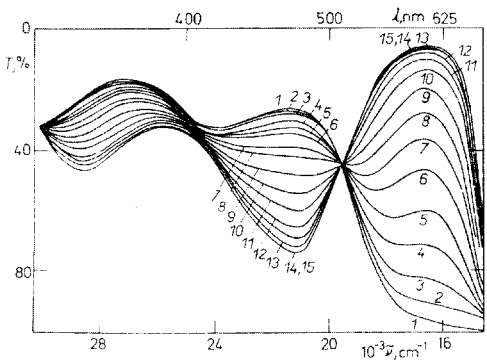

FIG. 5

The Absorption Curves of Cd(II) Solutions with TAMP in 30% v/v Ethanol

$c_M = 100$, $c_L = 4{\cdot}802 \cdot 10^{-3}$M, $I = 0{\cdot}10$, $t = 25{\cdot}00$°C, $d = 10$ mm. Curve — pH: *1* 3·20, *2* 3·68, *3* 4·18, *4* 4·50, *5* 4·77, *6* 4·95, *7* 5·11, *8* 5·28, *9* 5·47, *10* 5·71, *11* 5·95, *12* 6·26, *13* 6·72, *14* 7·15, *15* 8·02.

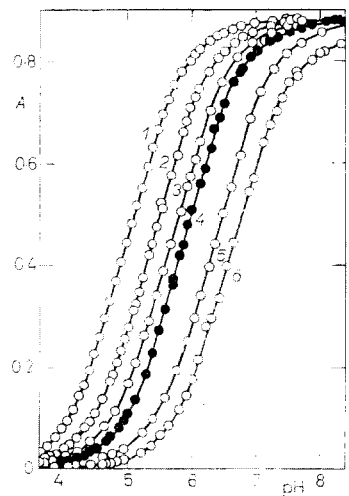

FIG. 6

The Absorbance–pH Curves for a Cd(II) Solutions with TAMP

$c_L = 4{\cdot}802 \cdot 10^{-5}$M, $\lambda = 595$ nm, for the other conditions see Fig. 5. Curve — c_M/c_L: *1* 250, *2* 100, *3* 50, *4* 30, *5* 10, *6* 5.

TABLE V

A Survey of Optical Characteristics of the Cd^{2+} Chelates with TAMP in 30% v/v Ethanol $I = 0{\cdot}10$, t 25°C.

c_M/c_L	$10^{-3}\,\nu_{max}$, cm^{-1}		$10^{-3}\,\nu_i$, cm^{-1}	λ_{max}, nm		λ_i, nm	$10^5 \cdot c_L$
100	25·8	16·6	19·5	388	602	513	4·802
1	26·0	16·7	19·6	385	599	510	4·802
1/10	25·2	17·0	19·8	397	588	505	24·01
5·71[a]	26·0	16·6	19·5	382	602	513	4·802

[a] Spectra recorded in dependence on the concentration excess of the cation at a constant pH of 5·71.

The concentration dependence curves, $A = f(c_M)$ and $A = f(c_L)$, increase uniformly for a constant low concentration of the components (c_L or c_M) and for several pH values in an interval of 4–7. Direct graphical analysis of curves $A = f(c_M)$, employing the $c_M^{-m} = f(1/A)$ dependence, gives a straight line for $m = 1$. When the $A = f(c_L)$ dependence is analyzed, function $c_L^{-n} = f[1/(A - A_L)]$ is practically linear for $n = 2$ and pH > 6, while in weakly acidic media the dependence is non-linear for any integral value of n. This fact again verifies the formation of complexes ML and ML_2 and shifts of the equilibrium toward the formation of the first or the second complex in solutions with excess cation or ligand, respectively.

The position of the absorption maximum on the continuous variation plots for pH = 5·5–7·5 and $c_0 = c_M + c_L = 9{\cdot}824 \cdot 10^{-5}$M at a mole fraction value of $x_L = c_L/(c_L + c_M) = 0{\cdot}55-0{\cdot}65$ also verifies the existence of a mixture of complexes ML and ML_2. With increasing pH value, complex ML_2 is formed preferentially.

Cadmium(II) *Complex with* TAMP

The spectra of the purple-blue reaction product of Cd^{2+} with TAMP in 30% v/v ethanol were measured under similar experimental conditions as those for Zn^{2+}. In solutions with excess cation and in equimolar solutions, the chelate exhibits two absorption bands, depending on the conditions, at 382–388 and 599–602 nm. Another maximum lies in the near UV region at 290–300 nm. The curves exhibit two sharp isosbestic points at 513 and 320 nm. In solutions with excess ligand, the maxima are affected by absorption of the ligand itself (forms LH and L^-); hence the assessment of the position of the absorption maximum is less precise. The λ_{max} values are slightly shifted to shorter wavelengths. The spectra at a constant pH, constant ligand concentration and varying cation concentration are analogous to those for excess metal. It again holds that only the curves for solutions with concentration

TABLE VI

A Survey of the Average Values of the Logarithm of the Equilibrium Constant of the Cd^{2+} Chelate with TAMP in 30% v/v Ethanol for Various Experimental Conditions (the component concentrations are identical with those given in Table VII)

c_M/c_L	$-\log {}^*\beta$	$-\log {}^*\beta^a$	$-\log {}^*\beta^b$	q^b	$r_{xy}{}^a$	$-\log {}^*\beta^a$	$r_{xy}{}^b$	$-\log {}^*\beta^b$	q^b
	pH_{inf}	graphical methods			the PRCEK II program				
250	3·02	3·02	3·02	0·994	0·9986	3·0278 ± 0·05770	0·9993	3·0205 ± 0·0230	0·9969
100	3·04	3·02	3·04	0·984	0·9972	3·0350 ± 0·06947	0·9977	3·0382 ± 0·0285	0·9882
50	3·04	3·03	3·04	0·984	0·9947	3·0306 ± 0·05721	0·9994	3·0169 ± 0·0443	1·0110
30	3·015	3·00	3·02	0·986	0·9973	3·0236 ± 0·06922	0·9994	3·0302 ± 0·0314	0·9963
10	3·03	3·01	3·02	0·989	0·9987	3·0340 ± 0·07247	0·9993	3·0371 ± 0·0801	0·9928
5	3·00	3·01	3·01	0·985	0·9990	3·0249 ± 0·08737	0·9988	3·0231 ± 0·0499	0·9718
≧ 5[c]	3·02	3·02	3·03	0·987	0·9979	3·0293 ± 0·04889	0·9990	3·0241 ± 0·0418	0·9927
1/2[d]	3·40	3·39	3·42	0·990	0·9993	3·3814 ± 0·09150	0·9981	3·2088 ± 0·0790	0·9761
1/2[e]	3·28	3·31	3·35	0·973	0·9852	3·1919 ± 0·17361	0·9729	3·2004 ± 0·5082	0·9166
1/10[f]	3·40	3·38	3·39	0·959	0·9983	3·3952 ± 0·27637	0·9979	3·3978 ± 0·2506	0·9606
1/20[e]	3·37	3·41	3·39	0·960	0·9992	3·4084 ± 0·33675	0·9968	3·4144 ± 0·5305	0·9971

[a] The results of direct graphical analysis using the $A = f(F_i)$ and $A = f(G_i)$ dependences, [b] the results of the graphical logarithmic analysis of the $\log F = f(pH)$ dependences, [c] the average from six values for 470, 560, 580, 595, 610 and 630 nm, [d] $c_M = 4{\cdot}80 \,.\, 10^{-5}$ M, the average from four values for 470, 630, 650 and 680 nm, [e] $c_M = 2{\cdot}401 \,.\, 10^{-5}$ M, the average from eight values for wavelengths of 470, 560, 580, 595, 600, 610, 630 and 680 nm, [f] the average from three values for 630, 650 and 670 nm.

ratios of $c_M/c_L \geqq 5$ pass through the isosbestic point. The curves at lower metal excesses do not pass through this point, presumably owing to the existence of a side equilibrium reaction (Table V).

The absorbance–pH curves for solutions with various concentration excesses of the metal ions ($c_M/c_L = 5 - 250$, $c_L = 4{\cdot}802 \cdot 10^{-5}$M) at a wavelength of 595 nm are given in Fig. 6. The curves are quite symmetrical and shift toward more acidic regions with increasing c_M/c_L values, thus indicating the existence of a single equilibrium and permitting direct determination of the A_{01}, A_{02} and $\log K_{mn}$ values from the horizontal branch and the position of the inflexion point; these values were employed as the

TABLE VII

A Survey of the Average Values of the Molar Absorption Coefficient of the Cd^{2+} Chelate with TAMP in 30% v/v Ethanol for Various Experimental Conditions

λ	Direct		Graphical		PRCEK program	
	ε_1	ε_2	ε_1	ε_2	ε_1	ε_2
470[a]	8 650	2 505	8 605	2 540	8 780 ± 16	2 369 ± 17
560[a]	570	14 270	525	14 015	632 ± 23	14 375 ± 24
580[a]	165	17 050[a]	90	17 870[a]	208 ± 32	17 091 ± 37
595[a]	130	17 945[a]	90	17 870[a]	96 ± 35	18 001 ± 39
600[a]	120	17 950[a]	80	17 950[a]	79 ± 42	18 036 ± 52
610[a]	110	17 265[a]	50	16 935	60 ± 37	17 025 ± 41
630[a]	60	14 675	20	14 720	37 ± 22	15 260 ± 29
650[a]	10	10 875	5	10 920	0 ± 12	11 095 ± 15
560[b]	—	—	11 950	19 520	11 719 ± 47	19 645 ± 555
580[b]	—	—	3 560	23 500	3 189 ± 110	23 645 ± 424
595[b]	1 250	31 000	1 220	29 890	1 189 ± 38	29 172 ± 284
600[b]	1 000	32 000	950	31 560	978 ± 47	31 604 ± 372
610[b]	750	32 000	680	31 490	742 ± 30	31 539 ± 430
630[b]	250	27 500	250	28 720	0 ± 16	28 546 ± 160
650[b]	0	20 000	40	20 100	0 ± 191	19 932 ± 310
680[b]	0	16 500	0	16 770	0 ± 61	16 671 ± 103
595[c]	0	17 950	25	17 885	0 ± 26	17 914 ± 73
600[c]	0	18 000	0	17 980	0 ± 34	17 978 ± 48
610[c]	0	17 250	0	17 370	0 ± 45	17 335 ± 52
630[c]	0	14 720	0	14 815	3 ± 29	14 833 ± 37
650[c]	0	10 950	0	11 030	0 ± 15	11 062 ± 43

[a] The results obtained from the absorbance–pH curves for $c_M/c_L > 3$, [b] the results obtained from the absorbance–pH curve for $c_L/c_M = 20$, [c] the results obtained from the $A = f(c_M)$ concentration dependences for a pH range of 5·0–6·5.

initial data for the graphical method and the PRCEK program. Graphical interpretation was performed for a wavelength of 595 nm and equilibria $(A)-(F)$, using the slope-intercept transformations, $A = f(F_i)$ or $A = f(G_i)$, under conditions identical with those for Zn^{2+}. The intercepts and slope (ε_1, ε_2 and $^*\beta_{mn}$) were evaluated by the least squares method. An $A = f(F_i)$ dependence for a hundredfold concentration excess of Cd^{2+} is shown in Fig. 7. Only the dependences for coefficients $mqn = 111$ and 211 and equilibria A and D are linear. The existence of complex M_2L was excluded by using the method of corresponding solutions, where the slope, m/q, of dependence $pH_{oi} = f(-\log c_M)$ equals approximately unity $(m/q = 0{\cdot}995)$.

Absorbances A_{01} and A_{02}, obtained from graphical analysis, were employed for the graphical logarithmic analysis of the curves. The evaluation was carried out by the least squares method only for the linear portion of curve $\log F = f(pH)$. Some of the results of the graphical methods are given in Tables VI and VII.

The reaction mechanism was selected from equilibria $(A)-(F)$ for a wavelength of 595 nm and concentration ratios c_M/c_L = 250, 100, 50, 30, 10 and 5, using the

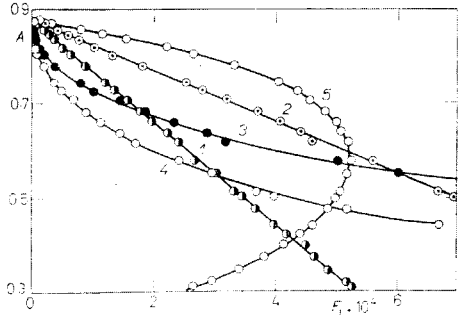

FIG. 7

Graphical Analysis of the Absorbance–pH Curves for Cd(II) Solution with TAMP

$c_M/c_L = 100$, $c_L = 4{\cdot}802 \cdot 10^{-5}$M, 595 nm, for the other conditions see Fig. 5. Curve — *mqn* coefficients — reaction:

1 111 — $M + LH = ML + H$,
2 211 — $2\,M + LH = M_2L + H$,
3 222 — $2\,M + 2\,LH = M_2L_2 + 2\,H$,
4 122 — $M + 2\,LH = ML_2 + 2\,H$,
5 112 — $M + 2\,LH = ML_2 + H$.

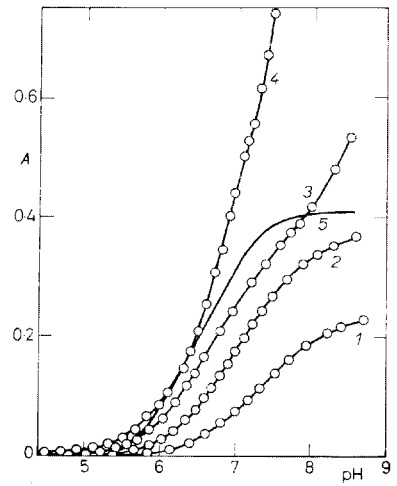

FIG. 8

The Absorbance–pH Curves for Cd(II) Solutions with TAMP for Various c_L/c_M Values

$c_M = 2{\cdot}401 \cdot 10^{-5}$M, for the other conditions see Fig. 5. Curve — c_L/c_M — $c_L \cdot 10^4$ — λ: *1* 5 — 1·200—680 nm, *2* 10 — 2·401 to 670 nm, *3* 20 — 4·802—670 nm, *4* 5 — 1·200 to 595 nm, *5* $\Delta A = A - A_L = f(pH)$ — 20 — 4·802—595 nm — modul $\Delta A = A/2$ (calculated).

PRCEK program with the criteria of the minimum sum of the squares of deviations U and the maximum value of correlation coefficient r_{xy}. Some of the results are given in Table VIII.

The values given verify unambiguously the conclusions made from the graphical methods, since the best U and r_{xy} values are always found for coefficients $mqn = 111$ and somewhat worse values for coefficients $mqn = 211$. In other cases the U and r_{xy} values lie outside the required limits ($U < 10^{-2}$, $r_{xy} \geqq 0{\cdot}995$). The molar absorption coefficients and equilibrium constants of reaction A were evaluated by the PRCEK program with the full number of iterations, $N_i \leqq 6$, from the values of the intercepts and the slope, using the least squares method, for all the wavelengths (470, 560, 580, 595, 600, 610 and 630 nm) and concentration ratios ($c_M/c_L = 250$, 100, 50, 30, 10 and 5). The results agree very well and the values obtained from the graphical and numerical methods are also in good agreement.

From graphical analysis of the absorbance–pH curves for solutions with excess ligand follows non-linearity of dependence $\Delta A = A - A_L = f(F_i \text{ or } G_i)$ under any

TABLE VIII

A Survey of the Values of the Correlation Coefficient, r_{xy}, and the Sum of the Squares of Deviations U for the Individual Reaction Mechanisms of the Formation of the Cd^{2+} Chelate with TAMP in 30% v/v Ethanol ($I = 0{\cdot}10$, $t = 25°C$, 595 nm, $c_L = 4{\cdot}802 \cdot 10^{-5}$M)

c_M/c_L	mqn	r_{xy}	$10^2 \cdot U$	r_{xy}^c	c_M/c_L	r_{xy}	$10^2 \cdot U$	r_{xy}^c
100	111	·99589	·1894	·99973	50	·99805	·1803	·99977
	112	·43243	133·7	·19142		·54153	1 149	·53743
	211	·99476	·1894	·99973		·81067	322·8	·99894
	122	·56066	241·6	·27071		·95440	72 381	·52230
	212	·56064	2 171	·27051		·03003	1 291	·29731
	222	·43243	305·5	·34878		·98739	1 814	·45472
5	111	·99850	·1199	·99950	1	·83244	423·5	·86929
	112	·73432	581·8	·82456		·71442	10 786	·83535
	211	·97551	1·346	·99398		·45947	149·1	·52411
	122	·96955	1 198	·77414		·87367	1·510	·88833
	212	·54993	57·49	·79908		·47977	164·2	·69275
	222	·98538	1 159	·80080		·86459	5 113	·90194
1/20[a]	111	·97579	1·406	·99452	1/20[ab]	·99956	·1878	·99971
	112	·94652	462·8	·92450		·80157	74·26	·72883
						·98290	9·525	·93597
	222	·91892	105·7	·90443		·93746	91·54	·95867
	133	·50637	36 459	·42762				

[a] $c_L = 4{\cdot}802 \cdot 10^{-4}$M, $c_M = 2{\cdot}401 \cdot 10^{-5}$M, [b] 680 nm, [c] the results of the graphical logarithmic analysis.

of the given conditions and for equilibria $(A)-(J)$. The correlation coefficients, r_{xy}, and the sums of the squares of the deviations do not fall in the required interval for any combination of coefficients mqn. The highest value of r_{xy}, 0·883, was found for $mqn = 111$, while the minimum value of U, $1{\cdot}5 \cdot 10^{-2}$, was obtained for $mqn = 122$.

Curves $A = f(F_i)$ and $A = f(G_i)$ for solutions with a ratio of $c_L/c_M = 20$ are linear for coefficients $mqn = 111$. The best r_{xy} and U values were also found by the PRCEK program for this combination, *i.e.* for equilibria (A) or (I). However, these values are not sufficient for evaluation of the linearity of the dependence ($r_{xy} = 0{\cdot}983$, $U = 1{\cdot}4 \cdot 10^{-2}$).

The characteristic parameters were obtained for coefficients $mqn = 111$ for all concentration ratios c_L/c_M and some wavelengths, which were selected individually for individual c_L/c_M values in order that the absorbance-pH curves exhibit at least slightly perceptible second horizontal branch, thus enabling assessment of the A_{02} value. The total absorbances of the solutions were corrected for the ligand dissociation and absorption by the LH and L^- forms and full number of iterations was carried out. The values of the chelate parameters vary considerably with variations

TABLE IX

The Resulting Values of the Equilibrium Constants, the Stability Constants and the Molar Absorption Coefficients

Quantity	Direct	Graph. Zn^{2+}	PRCEK II	Direct	Graph. Cd^{2+}	PRCEK II
$-\log^* \beta_{11}$ [a]	2·74	2·735	2·730 ± 0·04	3·02	3·025	3·025 ± 0·05
$-\log^* \beta_{11}$ [b]			2·735 ± 0·08			
$-\log \beta_{11}$	5·590	5·595	5·595 ± 0·06	5·30	5·30	5·30 ± 0·05
ε_{max} [c]	17 940	18 030	17 998 ± 71	17 950	17 950	18 040 ± 52
$-\log^* \beta_{12}$ [ae]	2·90	2·925	2·945 ± 0·15	3·39	3·40	3·40 ± 0·29
$-\log^* \beta_{12}$ [d]			2·99 ± 0·32			
$-\log \beta_{12}$	13·8	13·8	13·8 ± 0·2	13·3	13·3	13·3 ± 0·3
ε_{max} [c]	31 000	31 240	31 070 ± 210	32 000	31 560	31 605 ± 372

[a] The average value for the absorbance–pH curves, $A = f(pH)$, for 6 c_M/c_L values and 6 or 8 wavelengths, [b] the average of the values for the $A = f(c_M)$ curves and pH = 4·2—6·5, [c] 595 nm for Zn(II) and 600 nm for Cd(II), [d] the average value for $A = f(c_L)$ and pH 6·0, [e] the average for $c_L/c_M = 10$ (Zn^{2+}) or $c_L/c_M = 2, 10, 20$ (Cd^{2+}), $\beta_{mn} = {}^*\beta_{mn}/K_{ai}^n$

in the conditions and only at excesses $c_L/c_M \geqq 10$ partial agreement of equilibrium constant values is obtained ($^*\beta_{mn} = 0{\cdot}373 - 0{\cdot}413 \,.\, 10^{-3}$). This indicates again the presence of the side equilibrium for formation of complex ML_2.

CONCLUSION AND DISCUSSION

The results obtained for high excesses of zinc and cadmium ions show that a single complex, ML, is formed in a broad concentration range, $c_{Zn} = 10^{-4} - 5 \,.\, 10^{-3}$M and $c_{Cd} = 10^{-4} - 2 \,.\, 10^{-2}$M, at $c_L \approx 5 \,.\, 10^{-5}$M TAMP. It is formed in weakly acidic and neutral media by interaction of the molecular ligand form, LH, with the metal cation with dissociation of one proton, according to the scheme, $M + LH \rightarrow \rightarrow ML + H$. The formation of protonated complexes, MLH, ML_2H_2 *etc*,. which is common with dihydroxysubstituted azo-dyes (PAR, TAR *etc.*) and has been observed for the TAMP interaction with Hg^{2+} and Ni^{2+}, has not been found here, because of the pH value at which the Zn^{2+} and Cd^{2+} chelates exist[1,3].

In equimolar solutions and solutions with excess ligand ($c_M \simeq 3 \,.\, 10^{-5}$M, $c_L/c_M = 1 - 20$), a mixture of complexes ML and ML_2 with similar optical characteristics ($\lambda_{max} \simeq 600$ nm) is formed. At lower values of pH and the c_L/c_M ratio, chelate ML is preferentially formed, while chelate ML_2 is preferred at higher values. The higher chelate is formed by the interaction of the ligand LH form with the cation and also by conversion of the two chelates according to equations (*B*) and (*I*). Experimental conditions, under which only chelate ML_2 would be formed, were not found and thus the resulting molar absorbances and stability constants were derived from the results obtained for the highest concentration excess of the ligand (Table IX). The higher chelate is formed to a lesser extent for the two metals studied, compared to Ni^{2+}, Hg^{2+} and some other ions[1,3].

In comparison with other N-heterocyclic azo-dyes (derivatives of PAR, PAN, TAR, TAN *etc.*), TAMP and its derivatives appear to be unsuitable for direct spectrophotometric determination of Zn^{2+} and Cd^{2+}. The molar absorption coefficients and the colour contrast of the reaction are substantially better with a number of dyes ($\varepsilon_{560}^{PAN} \simeq 5{\cdot}6 \,.\, 10^4$ and $\varepsilon_{500}^{TAR} \simeq 3{\cdot}5 \,.\, 10^4$ for Zn^{2+} and $\varepsilon_{505}^{TAR} \simeq 3{\cdot}7 \,.\, 10^4$ and $\varepsilon_{560}^{PAN} \simeq (4{\cdot}7 - 5{\cdot}1) \,.\, 10^4$ for Cd^{2+}) (see refs[5-36]). Combination with extraction of the Zn^{2+} and Cd^{2+} chelates with the azo-dyes into organic solvents (benzene, chlorinated hydrocarbons, isopentylalcohol *etc.*) in a neutral or weakly alkaline region seems definitely more advantageous. Chelate ML_2^0 is extracted with TAMP and other ligands, while the anionic ligand form, L^-, remains in the aqueous phase. Hence a direct extraction-photometric method can be developed for the determination of the two ions.

REFERENCES

1. Kubáň V., Sommer L., Havel J.: This Journal *40*, 604 (1975).
2. Kubáň V., Havel J.: Acta Chem. Scand. *27*, 528 (1973).
3. Langová M., Havel J., Sommer L.: Chem. Anal. (Warsaw) *17*, 989 (1972).
4. Kubáň V.: *Thesis*. University of Brno 1972 .
5. Iwamoto T.: Bull. Chem. Soc. Japan *34*, 605 (1961).
6. Corsini A., Yih I. M., Fernando Q., Freiser H.: Anal. Chem. *34*, 1090 (1962).
7. Tanaka M., Funahashi S., Shirai K.: Inorg. Chem. *7*, 373 (1968).
8. Berger W., Elvers H.: Z. Anal. Chem. *171*, 185, 255 (1959); *199*, 166 (1964).
9. Betteridge D., Fernando Q., Freiser H.: Anal. Chem. *35*, 294 (1963).
10. Betteridge D., Todd R. K., Fernando Q., Freiser H.: Anal. Chem. *35*, 729 (1963).
11. Cheng K. L.: Anal. Chem. *30*, 243 (1958).
12. Nakagawa G., Wada H.: Nippon Kagaku Zasshi *83*, 1185 (1962), *84*, 639 (1963); Chem. Abstr. *59*, 9289 (1963), *61*, 1243 (1964).
13. Andrew T. R., Nichols P. N. R.: Analyst *90*, 161 (1965).
14. Galík A.: Talanta *16*, 201 (1969).
15. Chromý V., Sommer L.: Talanta *14*, 393 (1967).
16. Shibata S., Furukawa M., Sasaki S.: Anal. Chim. Acta *51*, 271 (1970).
17. Kawase A.: Talanta *12*, 195 (1965).
18. Kawase A.: Bunseki Kagaku *13*, 553 (1964); Chem. Abstr. *61*, 10100 (1965).
19. Yanagihara T., Matano N., Kawase A.: Trans. Nat. Res. Inst. Metals *2*, 56 (1960).
20. Kitano M., Ueda J.: J. Chem. Soc. Japan, Pure Chem. Sect. *91*, 983 (1970).
21. Gusev S. I., Nikolajeva E. M., Pirožkova E. A.: Ž. Anal. Chim. *26*, 1740 (1971).
22. Gusev S. I., Žvakina M. V., Koževnikova I. A.: Ž. Anal. Chim. *26*, 1493 (1971).
23. Shibata S., Furukawa M., Ishiguro Y.: Mikrochim. Acta *1972*, 721.
24. Adamovič L. P., Geršuns A. L., Olejnik A. A., Škabara N. M.: Ž. Anal. Chim. *26*, 548 (1971).
25. Klotz I. M., Loh-Ming W. C.: J. Am. Chem. Soc. *75*, 4159 (1953).
26. Navrátil O.: This Journal *29*, 2490 (1964).
27. Hniličková M., Sommer L.: This Journal *26*, 2189 (1961).
28. Hniličková M., Sommer L.: Talanta *13*, 667 (1966).
29. Havíř J., Vřešťál J.: Chem. Listy *60*, 64 (1966).
30. Püschel R.: Z. Anal. Chem. *221*, 132 (1966).
31. Cheng K. L., Bray R. H.: Anal. Chem. *27*, 782 (1955).
32. Stanley R. W., Cheney G. E.: Talanta *13*, 1619 (1966).
33. Nickles G., Pollard F. H., Samuelson T. J.: Anal. Chim. Acta *39*, 469 (1967).
34. Talipov S. T., Džambajeva R. Ch., Charpasova L. V., Gutnikova R. J.: Nauč. Trudy Tašk. Univ. No *263*, 72 (1964); Chem. Abstr. *62*, 15425 (1966).
35. Drapkina D. A., Brudz V. G., Smirnova K. A., Dorošina N. J.: Ž. Anal. Chim. *17*, 940 (1962).
36. Škrobot E. P., Banikovskaja L. M.: Zavod. Lab. *32*, 1452 (1966).

Translated by M. Štuliková.